ACS OMEGA

Open Access

http://pubs.acs.org/journal/acsodf

Article

Structural Evolution Study of Titanium−Vanadium−Niobium Nanoparticles from Single to Multicomponent Systems

Yi-Rong Liu,* Yan Jiang, and Lang Bai

Cite This: *ACS Omega* 2024, 9, 45545−45553

Read Online

ACCESS | Metrics & More | Article Recommendations | Supporting Information

ABSTRACT: In this article, the revised basin-hopping with mirror-rotation sampling combined with density functional theory, which was proposed by our previous study, was used to study the structural property of Ti_n ($n = 3m$, $m = 1−7$), V_n ($n = 3m$, $m = 1−7$), Nb_n ($n = 3m$, $m = 1−7$), and $Ti_nV_nNb_n$ ($n = 1−7$) systems. We found that equiatomic $Ti_nV_nNb_n$ ($n = 1−7$) systems do not change their lowest energy structures relative to the same size Ti_n ($n = 3m$, $m = 1−7$), V_n ($n = 3m$, $m = 1−7$), and Nb_n ($n = 3m$, $m = 1−7$) systems, and this indicates that the nanoparticles composed of titanium, vanadium, or niobium elements may have similar energy morphologies when the atomic number is the same. Based on the low-energy structural similarity of titanium−vanadium−niobium systems between single and multicomponent, we used the element space position replacement (ESPR) method to reconstruct the low-energy structure of $Ti_nV_nNb_n$ ($n = 1−7$) systems. For the $Ti_7V_7Nb_7$ system, the average sampling step of 10 separate searches of the BH-MRS method is 1226 more than that of the ESPR method to find the lowest energy structure (six-ring layered structure). The electronic property calculation shows that using equiatomic vanadium and niobium elements to replace titanium element in the Ti_n ($n = 3m$, $m = 1−7$) system may not change its stability, and the Ti_n ($n = 3m$, $m = 1−7$) system has better electron trapping ability than V_n ($n = 3m$, $m = 1−7$), Nb_n ($n = 3m$, $m = 1−7$), and $Ti_nV_nNb_n$ ($n = 1−7$) systems. Our method and results can be helpful for the design of nanostructures of transition metals with better catalytic properties.

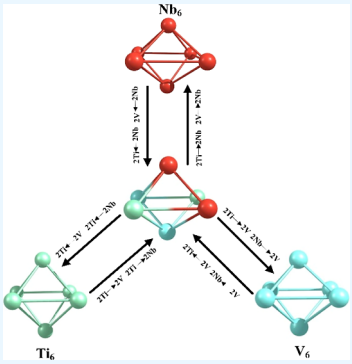

INTRODUCTION

Transition metals (TMs) have been a hot research topic due to their unique physicochemical properties.[1−4] These unique properties arise from their open d-shell electronic structure, and so, they are used in many fields, for example, nanomaterials, catalysis, high-entropy alloys (HEAs), and so on. At the nanoscale, TM clusters have also been studied extensively since they have unique quantum chemical effects and can be seen as a minimum functional structure primitive for constructing special material devices, such as catalyst, hydrogen storage material, and microelectronics devices.[5,6] Therefore, studying the structure−property relationship of TM clusters at the molecular level is very helpful to design different functional materials.

An important application of these transition metals is the HEAs, and their composition mainly contains Ti, V, Nb, Zr, Ni elements, and so on. Over the past two decades, the HEAs have attracted much attention from materials researchers due to their unique mechanical properties relative to traditional alloys.[7−9] All of the elements that form the HEAs are solidly dissolved into a single phase after quenching, and these elements are uniformly and randomly distributed in the lattice. This property makes the HEAs have better mechanical properties than the traditional alloy in the middle and high-temperature region.[10,11] Due to strong s and d orbital interactions of these TM elements, their interaction mechanism of structure−activity relationship remain unsolved for multicomponent TM systems at the molecular level. Different experimental techniques have been used to study the stability and dissociation energy of these TM clusters, such as photoelectron spectroscopy,[12] time-of-flight (TOF) mass spectroscopy,[13] and high-resolution electron microscopy.[14] However, these methods can not directly give the structure−physicochemical property relationship of TM clusters. Therefore, theoretical calculation will be a very important tool for us to predict the structure evolution process of these TM clusters. Our previous theoretical calculation showed that the equiatomic vanadium−titanium-mixed clusters do not change their ground-state structure relative to the same size pure vanadium and titanium cluster.[15] This indicates that swapping the spatial coordinates of these elements does not change their structure, and this may provide an effective solution for the design of multicomponent structures. In the last two decades, different theoretical methods have also been used to predict the physicochemical and mechanical properties of HEAs, such as empirical models,[16] first-principles calculations,[17] calculation

Received: August 22, 2024
Revised: October 22, 2024
Accepted: October 24, 2024
Published: October 30, 2024

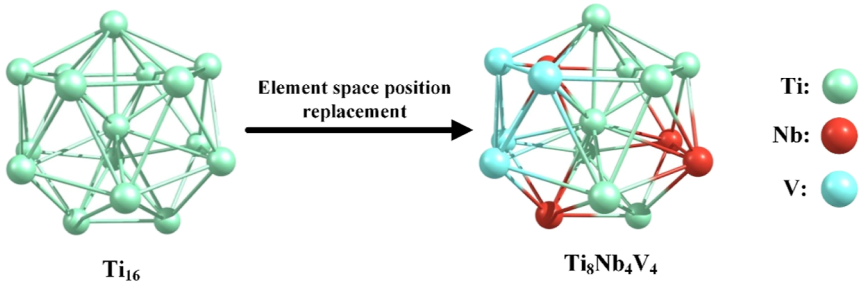

Figure 1. Schematic diagram of structure designing of multicomponent systems by element space position replacement based on the low-energy structure of single-component systems.

of phase diagrams,[18] machine learning algorithms,[19] and so on.[20] These methods can greatly reduce the trial and error cost of the experimental process and are an important tool for the future design of HEAs.

For the nanoscience field, the structure of nanoparticles is the basis of studying their physical and chemical properties and is also a bridge between macroscopic materials and microscopic structures. Therefore, global minima (GM) searching based on fixed elemental composition and size has become an important scientific problem for cluster or nanoscience. For the past 20 years, different GM searching algorithms, such as basin-hopping,[21] genetic algorithm,[22] simulated annealing,[23] and particle swarm optimization,[24] have been proposed to solve the tough problem. However, for multicomponent systems, because it involves the exchange of spatial positions between different elements, the difficulty of GM searching will be further increased. For this problem, our previously proposed BH-MRS method can effectively solve the structure searching problem of multicomponent TM clusters.[15,25]

Based on our previous focus on the vanadium−titanium alloy field, we will further extend the study to the more complex ternary system of TiVNb, where the ratio of titanium−vanadium−niobium is always 1:1:1 as the base component to produce a medium-entropy alloy. Ti, V, and Nb are the common elements that make up of the HEAs,[26−31] and the study of their microstructure will help us to further understand the formation mechanism of HEAs at the molecular level. In this paper, we will use the previously proposed BH-MRS method combined with density functional theory to explore the structure evolution process of Ti_n (n = 3m, m = 1−7), V_n (n = 3m, m = 1−7), Nb_n (n = 3m, m = 1−7), and $Ti_nV_nNb_n$ (n = 1−7) systems.

METHODS

BH-MRS Algorithm. For multicomponent TM systems, exchanging spatial positions of different elements in the cluster will change the energy of the system and can be regarded as local searching on potential energy surface (PES). The BH-MRS method, which was proposed by our previous study, is very effective for global minima (GM) searching of multicomponent systems by our previous study. The generalized basin-hopping is also a very effective method for the structure searching of multicomponent systems by focusing on biminima, which is proposed by Wales and Schebarchov to describe these special local minima points on the PES for multicomponent systems.[32] For these transition metal (TM) systems, the Perdew−Burke−Ernzerhof (PBE) exchange−correlation functional[33] and the double-numerical polarized (DNP) basis set were used for the geometric optimization in the DMol^3 code.[34] The PBE functional combined with the DNP basis set can effectively describe the structural properties of TM systems as described in previous studies. The parameter setting for configuration optimization is 2×10^{-5} hartree for energy convergence, 0.005 Å for gradient convergence, and 0.004 Å for displacement convergence. The spin polarization restriction and symmetry constraints are not used for these TM elements. The mirror parameter (l) is set to l = 0.78, and the range of rotation angle is from 0 to π. Five independent BH-MRS tasks, consisting of 1000 sampling with randomly generated initial structures, were performed for each cluster. When all of 5000 isomers with different energies were obtained by the BH-MRS algorithm, and then they were ranked according to their relative energies. The relative energies were calculated by the difference between the global minimum (GM) and the local minimum (LM) for five separate searching, $\Delta E = E(\mathrm{LM}) - E(\mathrm{GM})$. Note that the GM was selected by collection sort that collect all different minima from five separate searching and select the GM to calculate energy differences with respect to the GM. The low-energy candidates selected within 6 kcal/mol relative to GM were reoptimized at the Orca software package using the RPBE functional with different basis sets for these TM elements, the TZVP basis set for Ti and V elements, and the LANL2DZ basis set for Nb element.[35]

Element Space Position Replacement Method. Our previous studies have shown that the equiatomic vanadium−titanium systems have a similar low-energy structure with pure titanium and vanadium systems. This means that the low-energy structure of equiatomic vanadium−titanium systems can be constructed using the low-energy structure of pure titanium or vanadium systems by replacing half of titanium or vanadium with vanadium or titanium (Ti → V or V → Ti), which greatly reduces the structure searching time and improves the efficiency of structure design. Therefore, based on the above structural characteristic, we used another structure generation method of multicomponent transition metal (TM) nanoparticles named element space position replacement (ESPR) for $Ti_nV_nNb_n$ (n = 1−7) system searching. The low-energy structure of $Ti_nV_nNb_n$ (n = 1−7) systems will be explored by ESPR and BH-MRS methods, independently. For the ESPR method, it constructed the structure of $Ti_nV_nNb_n$ (n = 1−7) systems based on the low-energy configurations of single-component systems with the same number of atoms. Figure 1 shows the schematic diagram of ESRP, and the coordinates of relevant elements in the single-component structure are randomly replaced by other elements to generate local minima on the structural space of multicomponent systems. Expression 1 represents the sampling transformation from the low-energy configuration of single-

https://doi.org/10.1021/acsomega.4c07777
ACS Omega 2024, 9, 45545−45553

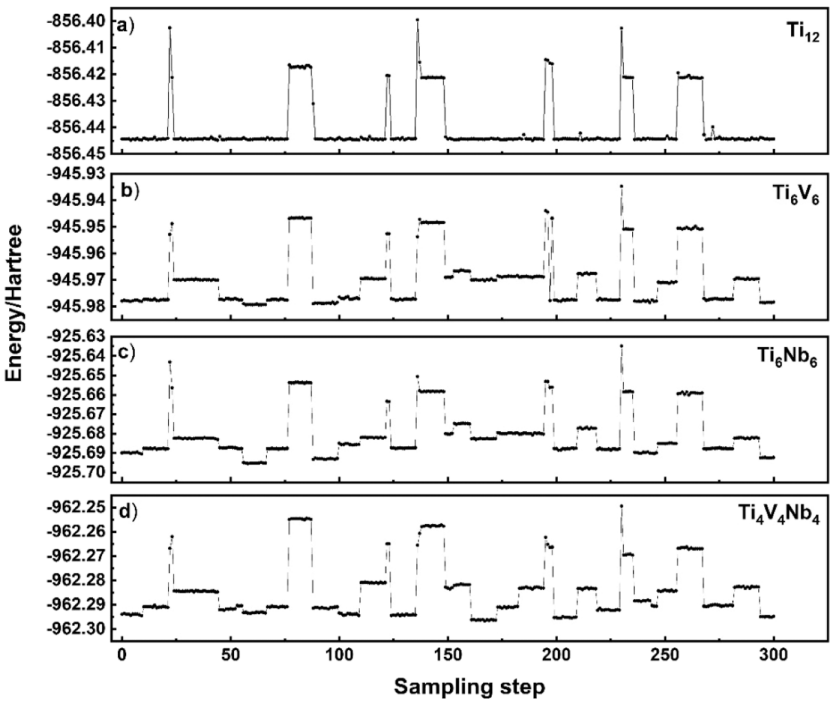

Figure 2. Change trend of energy-sampling step for (a) Ti_{12}, (b) Ti_6V_6, (c) Ti_6Nb_6, and (d) $Ti_4V_4Nb_4$ systems. Note that the generation of low-energy structure of Ti_6V_6, Ti_6Nb_6, and $Ti_4V_4Nb_4$ systems by the transformation of V and Nb element replacement based on the fixed Ti_{12} cluster.

component to the multicomponent structural space, where the symbol $\hat{T}$ represents the exchange operation, R and R' represent the position of structural space for single and multicomponent systems, x represents the Cartesian coordinates of the atoms, and α, β, and γ represent the element type. Note that the space position R at the PES of single-component systems must also satisfy Expression 2, where the partial derivative of the potential function E^{α} with respect to the structure R is zero. This indicates that R is an element in the set of local minima on the PES of one-component systems. Therefore, the generation of multicomponent structures is based on these local minimum points on the PES of single-component systems.

$$\hat{T}(R(x_1^{\alpha}, x_2^{\alpha}, \ldots\ldots, x_{n-1}^{\alpha}, x_n^{\alpha})) = R'(x_1^{\alpha}, x_2^{\alpha}, \ldots\ldots, x_{k-1}^{\beta}, x_k^{\beta}, \ldots\ldots, x_{n-1}^{\gamma}, x_n^{\gamma}) \quad (1)$$

$$\frac{\partial E^{\alpha}}{\partial R} = 0 \quad (2)$$

RESULTS AND DISCUSSION

Structure Invariant from Single to Multicomponent. In order to demonstrate that random replacement of atomic coordinate positions in a fixed single-component structure with different elements does not affect the structure, we take the Ti_{12} cluster as an example and use the BH-MRS method to search its low-energy structure on the PES. The results are shown in Figure 2a, and note that these points on the diagram represent the local minimum (LM) on the PES of the Ti_{12} system. Figure 2b,c represents the generation of the low-energy structure of binary Ti_6V_6 and Ti_6Nb_6 systems by the transformation of Expression 1 (ESPR) based on the corresponding fixed structure in Figure 2a. For each transformation in Figure 2b,c, six atoms of each corresponding Ti_{12} structure are randomly replaced by the V and Nb elements. The configuration optimization is required after the replacement operation to confirm that the structure is a local minimum on the PES. As the same operation above, the low-energy structures of the $Ti_4V_4Nb_4$ system at Figure 2d were obtained by the transformation of Expression 1 (ESPR). When comparing the changes from Figure 2a–d, we can find that the evolutionary trends of energy-space structure are very similar for single-component (Ti_{12}), two-component (Ti_6V_6, Ti_6Nb_6), and three-component ($Ti_4V_4Nb_4$) systems. This indicates that replacing titanium with vanadium or niobium elements does not change their structure for the Ti_{12} system. In addition, the structural similarity between each sampling point has also been compared quantitatively using ultrafast shape recognition (USR) algorithm for Ti_{12}–Ti_6V_6, Ti_{12}–Ti_6Nb_6, and Ti_{12}–$Ti_4V_4Nb_4$ systems,[36−39] and the results at Figure 3 show that all of structure similarity values are greater than 0.9 (larger than 0.9 is considered similar and greater than 0.95 is considered very similar). The similarity between structures can be calculated using Expression 3.

$$S_{ij} = \left(1 + \frac{1}{12}\sum_{l=1}^{12}(|M_l^i - M_l^j|)\right)^{-1} \quad (3)$$

where M_l^i and M_l^j are the lth descriptors for structures i and j, respectively. The closer S_{ij} is to 1.0, the more similar the two structure are. The descriptors M_l^i for structure i can be calculated by $\vec{M} = (\mu_1^{ctd}, \mu_2^{ctd}, \mu_3^{ctd}, \mu_1^{cst}, \mu_2^{cst}, \mu_3^{cst}, \mu_1^{fct}, \mu_2^{fct}, \mu_3^{fct}, \mu_1^{ftf}, \mu_2^{ftf}, \mu_3^{ftf})$ which the ctd represents the molecular centroid, the cst represents the closest atom to the ctd, the fct represents the farthest atom from the ctd, and the ftf represents the farthest atom from the fct. The details of structural similarity calculations can be found in our previous study.[15] Note that

https://doi.org/10.1021/acsomega.4c07777
ACS Omega 2024, 9, 45545−45553

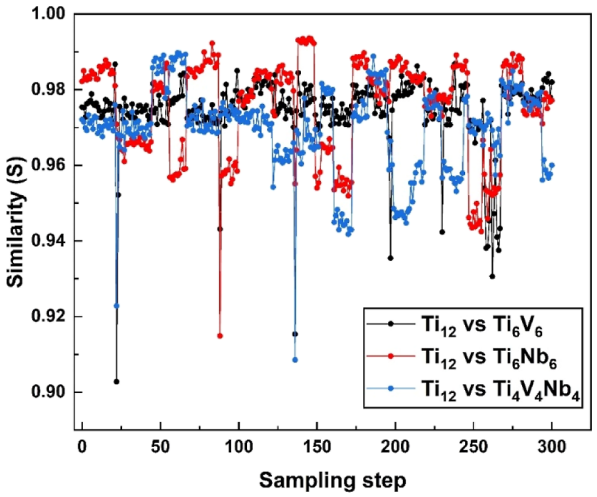

Figure 3. Similarity comparison of the low-energy structures of Ti_{12}, Ti_6V_6, Ti_6Nb_6, and $Ti_4V_4Nb_4$ systems using the USR algorithm with a normalized average bond length of 2.0 Å.

before the similarity calculation using the USR algorithm, we normalized the average bond length to 2 Å for evaluating the similarity. Therefore, based on the above analysis and calculations, we can reasonably infer that the nanoparticles composed of titanium, vanadium, or niobium elements have similar energy morphologies when the atomic number is the same. We now define a condition for this property of the TiVNb system that satisfies

$$\frac{\partial E^I}{\partial R} = 0 \tag{4}$$

where E^I represents the energy function with the same atomic number and I is the set of element types ($I \in$ {Ti, V, Nb, TiV, TiNb, VNb, and TiVNb}). R represents the same configuration for the energy functions of different components.

Structural Analysis. In order to study the structural characteristics of TiVNb systems at the molecular scale, we use both ESPR and BH-MRS methods described in the method section to search the low energy structures of equiatomic $Ti_nV_nNb_n$ (n = 1−7) systems. First, the low-energy structures of Ti_n (n = 3m, m = 1−7), V_n (n = 3m, m = 1−7), and Nb_n (n = 3m, m = 1−7) clusters were obtained using the BH-MRS method proposed by our previous study. For each cluster, 10 separate BH-MRS searching were performed, and each searching contained 600 structures. Then, these isomers were ranked according to their relative energies, which were calculated by the difference between the global minima (GM) and the local minima (LM). The low-energy candidates selected within 3 kcal/mol relative to GM, and the GM structures of Ti_n (n = 3m, m = 1−7), V_n (n = 3m, m = 1−7), and Nb_n (n = 3m, m = 1−7) systems are shown at Figure 4 (three columns left). Second, based on these low-energy candidates of Ti_n (n = 3m, m = 1−7), V_n (n = 3m, m = 1−7), and Nb_n (n = 3m, m = 1−7) systems, we use the ESPR method to explore the low-energy structure of equiatomic $Ti_nV_nNb_n$ (n = 1−7) systems, and the GM structures are shown in Figure 4 (rightmost).

For Ti_n (n = 3m, m = 1−7) clusters, the GM structures of Ti_6, Ti_{12}, and Ti_{18} cluster are consistent with those previously reported, and the low-energy structures of Ti_3, Ti_9, Ti_{15}, and Ti_{21} cluster were studied using the mirror-rotation sampling (MRS) method for the first time. The GM structure of the Ti_3 cluster is a standard equilateral triangle. For the Ti_9 cluster, the lowest energy structure is formed by adding one Ti atom to a plane of the ground-state Ti_8 structure. Our previous study shows that the GM structure of M_{N+1} usually can be constructed by adding one or two atoms on some plane of the low-lying isomers of M_N.[40] This is very consistent with the principle of minimization of structure matching polymerization proposed by our previous study.[41] Based on the same principle, the ground-state structures of Ti_{15} and Ti_{21} can be regarded as the lowest energy structures of Ti_{14} and Ti_{20} clusters adsorbing one Ti atom, respectively.

The ground-state structures (see Figure 4) of V_n (n = 3m, m = 1−7) and Nb_n (n = 3m, m = 1−7) systems are very similar to that of Ti_n (n = 3m, m = 1−7) systems except for the Nb_6 cluster molecule. Although the lowest energy structure of Nb_6 is different from the same size pure titanium and vanadium, a similar structure can be found at slightly higher low-energy isomers relative to the ground-state structure of Nb_6. Previous experimental studies have shown that the low-lying and lowest energy isomer can coexist at finite temperature. Therefore, we can infer that the ground-state structures of different sizes may come from the adsorption superposition of the smaller low-energy configurations with single or double atoms for V_n (n = 3m, m = 1−7) and Nb_n (n = 3m, m = 1−7) systems, and this result is consistent with our previous research.

For the ternary $Ti_nV_nNb_n$ (n = 1−7) systems at Figure 4, almost all the lowest energy structures are very similar to the same size pure titanium, vanadium, and niobium cluster (rightmost), and the results in Figure 5 show that more than 81% structure similarity values are greater than 0.9 (larger than 0.9 is considered similar). Note that the GM structure of $Ti_6V_6Nb_6$ is different from the same size Ti_{18}, V_{18}, and Nb_{18} cluster, but a similar structure can be found at slightly higher low-energy isomers relative to the ground-state structure of $Ti_6V_6Nb_6$. If we use the low-energy structure of the $Ti_6V_6Nb_6$ cluster molecule to calculate the similarity with the GM structure of Ti_{18}, V_{18}, and Nb_{18} molecules, and their structural similarity values will be 0.95, 0.97, and 0.96, respectively. Based on the structure and similarity analysis, we found that equiatomic titanium−vanadium−niobium systems do not change their lowest energy structures relative to the same size pure titanium, vanadium, and niobium cluster. Therefore, the addition of the niobium element does not change the ground-state structures of titanium−vanadium mixed systems at the molecular level, which indicates that niobium can be used as an important element of HEAs. Because the spatial position of each element in the lattice of the single-phase HEAs is randomly distributed. Our previous experimental results by XRD characterization show that adding niobium element to pure titanium or vanadium metals does not change their microstructure, and they have the same BCC structure for equiatomic TiVNb, V_2Nb, and Ti_2Nb alloys.[15] The structure analysis based on our theoretical calculation for the ternary $Ti_nV_nNb_n$ (n = 1−7) systems is in agreement with previous experimental measurement.

In order to demonstrate the effectiveness of the ESPR method, we have performed an unbiased search of the ternary $Ti_4V_4Nb_4$ system using the BH-MRS method (see Figure 6). We found that the lowest energy structure of the $Ti_4V_4Nb_4$ system obtained by the BH-MRS method was consistent with that of the ESPR method, which indicates that the ESPR method has a very significant advantage in the rapid

https://doi.org/10.1021/acsomega.4c07777
ACS Omega 2024, 9, 45545−45553

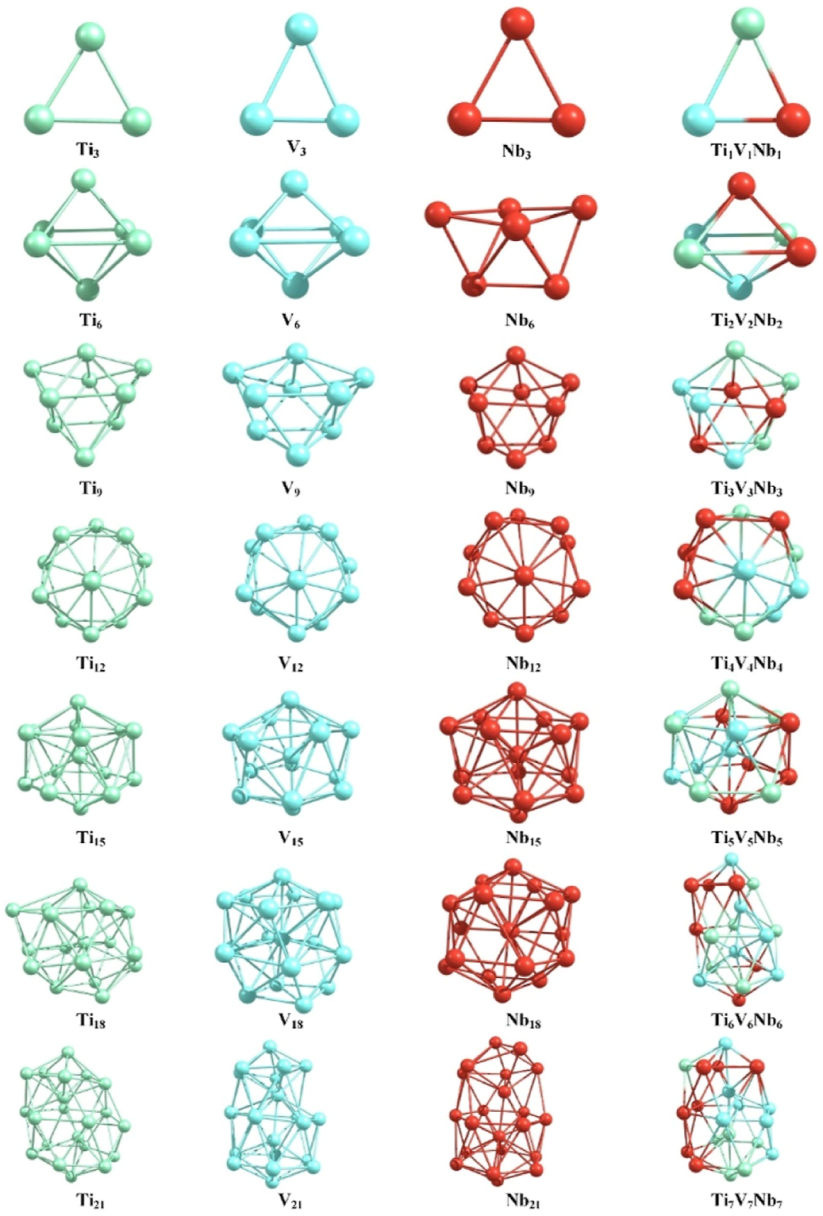

Figure 4. Lowest energy structures of Ti_n ($n = 3m$, $m = 1-7$), V_n ($n = 3m$, $m = 1-7$), Nb_n ($n = 3m$, $m = 1-7$), and $Ti_nV_nNb_n$ ($n = 1-7$) systems. The green, cyan, and red atoms represent titanium, vanadium, and niobium, respectively.

construction of low-energy structures of multicomponent nanoparticles.

Comparison of the ESPR and BH-MRS Method. In order to compare the difference of the ESPR and MRS-Swap method in the global structure searching of multicomponent nanoparticles, we have first performed 15 separate unbiased global structure searches for the $Ti_7V_7Nb_7$ system using the BH-MRS method, consisting of 5000 sampling steps at the MRS process for each searching. The GM structure of the $Ti_7V_7Nb_7$ system is a typical six-ring layered structure, and so it will be a good example for the test. Figure 7 shows the number of quenches required for finding the global minima of the $Ti_7V_7Nb_7$ system using the BH-MRS method for 15 independent runs, and the average quenching number is 945 steps for 10 independent BH-MRS searching. On the contrary, the starting point of the searching $Ti_7V_7Nb_7$ system using the ESPR method is the fixed six-ring layered structure of the V_{21} system. Figure 8a shows that the sampled configuration energy versus the sampling count for the $Ti_7V_7Nb_7$ system use the ESPR method based on the fixed six-ring layered structure of the V_{21} cluster molecule. The similarity (see Figure 8b) of these low-energy structures of the $Ti_7V_7Nb_7$ system and the six-ring-layered structure of the V_{21} cluster molecule was also compared using the USR algorithm with a normalized average bond length of 2.0 Å, and the results (see Figure 8b) show that all of structure similarity values are greater than 0.9 (larger than 0.9 is considered similar), and more than 97.5% structure similarity values are greater than 0.95 (larger than 0.95 is considered extremely similar). Based on the above analysis, we found that the ESPR method is 945 sampling steps faster than the BH-MRS method on average to find the six-ring layered structure, and the similarity calculation indicates that the $Ti_7V_7Nb_7$ system has structure invariance for element exchange at the molecular level. Therefore, the ESPR method is more efficient than the BH-MRS method in the global minimum searching of $Ti_nV_nNb_n$ ($n = 1-7$) systems.

https://doi.org/10.1021/acsomega.4c07777
ACS Omega 2024, 9, 45545−45553

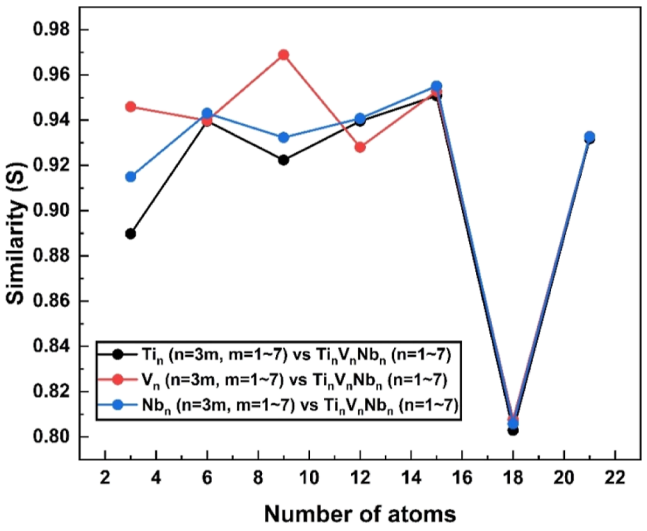

Figure 5. Similarity comparison of the GM structures of Ti_n ($n = 3m$, $m = 1-7$), V_n ($n = 3m$, $m = 1-7$), Nb_n ($n = 3m$, $m = 1-7$), and $Ti_nV_nNb_n$ ($n = 1-7$) systems using the USR algorithm with a normalized average bond length of 2.0 Å.

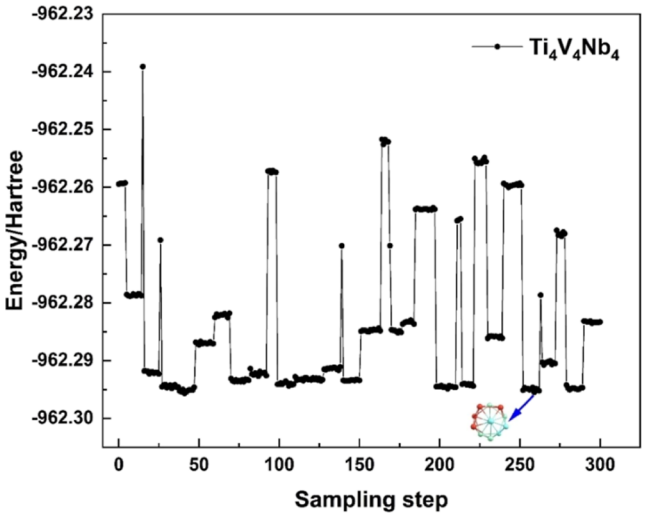

Figure 6. Global structure searching for the $Ti_4V_4Nb_4$ system using the BH-MRS method. The blue arrow represents the global minima (GM).

Electronic Properties. In order to further characterize the relative stability of Ti_n ($n = 3m$, $m = 1-7$), V_n ($n = 3m$, $m = 1-7$), Nb_n ($n = 3m$, $m = 1-7$), and $Ti_nV_nNb_n$ ($n = 1-7$) systems, the binding energies of their GM clusters are calculated by eqs 5 and 6

$$E_b(\text{single component}) = \frac{(E_{total} - NE_{atom})}{N} \quad (5)$$

where E_{total} represents the total energy of Ti_n, V_n, and Nb_n systems and E_{atom} is the single-atom energy for Ti, V, and Nb. N is the number of atoms in a cluster.

$$E_b(\text{multicomponent}) = \frac{(E_{total} - NE^{Ti}_{atom} - NE^{V}_{atom} - NE^{Nb}_{atom})}{3N} \quad (6)$$

where E_{total} represents the total energy of the $Ti_nV_nNb_n$ system, and E_{atom} is the single-atom energy for Ti, V, and Nb. $3N$ is the number of atoms in a cluster. Figure 9 shows that the binding energy increases with the cluster size, and their trends are very similar, which may be caused by their structural similarity discussed at above. We note that the binding energy curves of Ti_n ($n = 3m$, $m = 1-7$) and $Ti_nV_nNb_n$ ($n = 1-7$) systems almost coincide, and this may be due to the fact that the increase and decrease of the binding energy by niobium and vanadium elements in $Ti_nV_nNb_n$ ($n = 1-7$) systems just offset each other. Therefore, adding equiatomic vanadium and niobium elements to a pure titanium system may not change its stability, which provides theoretical guidance for further design of HEAs with better mechanical properties.

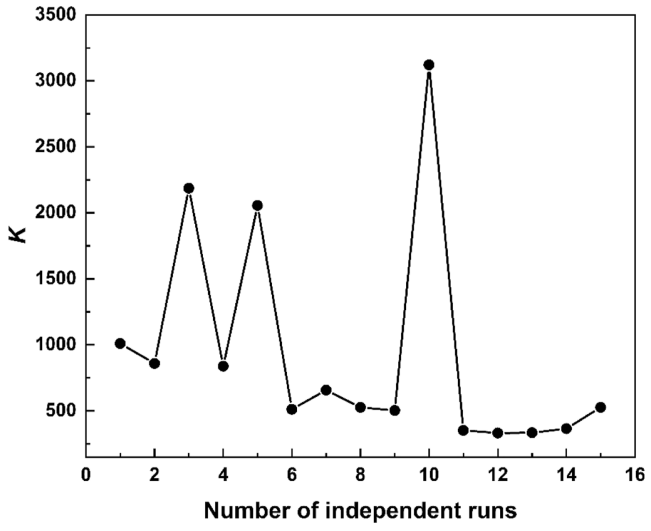

Figure 7. Number of quenches (K) required for finding the global minima (six-ring layered structure for the $Ti_7V_7Nb_7$ system) versus 15 independent runs for the BH-MRS method. The initial structure is random for each run.

To further study the electronic structural property of Ti_n ($n = 3m$, $m = 1-7$), V_n ($n = 3m$, $m = 1-7$), Nb_n ($n = 3m$, $m = 1-7$), and $Ti_nV_nNb_n$ ($n = 1-7$) systems, we calculated their vertical ionization potential (VIP) and vertical electron affinity (VEA). The VIP and VEA are calculated as follows

$$\text{VIP} = E(\text{cation at optimized neutral structure}) - E(\text{optimized neutral structure}) \quad (7)$$

$$\text{VEA} = E(\text{optimized neutral structure}) - E(\text{anion at optimized neutral structure}) \quad (8)$$

Recently, HEAs have received extensive attention in the field of catalysis due to its unique active sites.[42−45] Therefore, calculating the electronic structural properties of HEAs can help us to understand their catalytic properties at the molecular level. The simulations of VIP and VEA are plotted in Figure 10 for Ti_n ($n = 3m$, $m = 1-7$), V_n ($n = 3m$, $m = 1-7$), Nb_n ($n = 3m$, $m = 1-7$), and $Ti_nV_nNb_n$ ($n = 1-7$) systems. The results show (Figure 10a) that the average VIP of Nb_n ($n = 3m$, $m = 1-7$) systems (4.93 eV) is larger than that of Ti_n ($n = 3m$, $m = 1-7$) (4.57 eV), V_n ($n = 3m$, $m = 1-7$) (4.84 eV), and $Ti_nV_nNb_n$ ($n = 1-7$) (4.63 eV) systems and gradually decreases for all of systems when the number of atoms increases. This indicates that these systems will become more and more easy and unstable to lose electrons as the size increases. On the contrary, the ability of capturing electrons

https://doi.org/10.1021/acsomega.4c07777
ACS Omega 2024, 9, 45545−45553

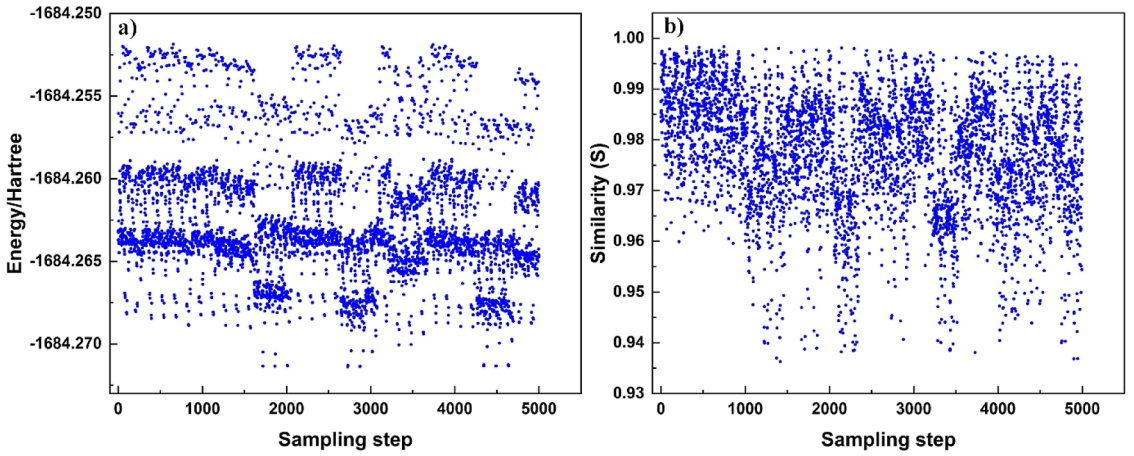

Figure 8. Structure searching of the $Ti_7V_7Nb_7$ system by the ESPR method based on the fixed six-ring layered structure of the V_{21} cluster molecule: (a) sampled configuration energy versus the sampling count for the $Ti_7V_7Nb_7$ system and (b) similarity comparison of the sampled configuration of the $Ti_7V_7Nb_7$ system by the ESPR method and the fixed six-ring layered structure of the V_{21} cluster molecule using the USR algorithm with a normalized average bond length of 2.0 Å.

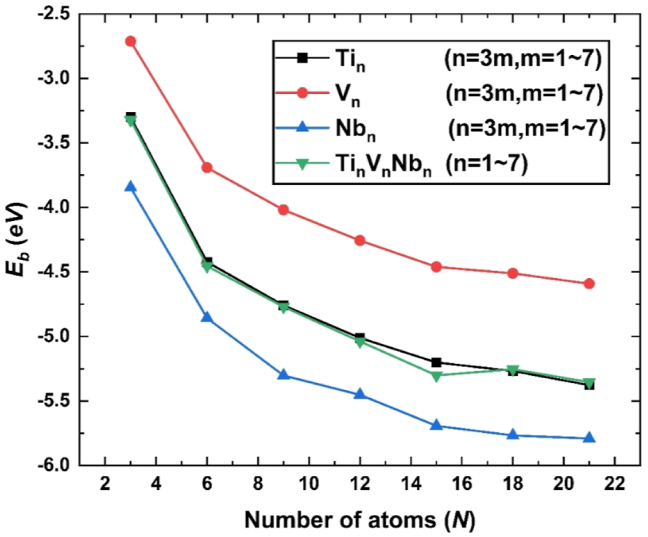

Figure 9. Binding energy of the GM for Ti_n ($n = 3m$, $m = 1-7$), V_n ($n = 3m$, $m = 1-7$), Nb_n ($n = 3m$, $m = 1-7$), and $Ti_nV_nNb_n$ ($n = 1-7$) systems.

gets better and better as the size increases for all of the systems shown at Figure 10b, and the average VEA for Ti_n ($n = 3m$, $m = 1-7$), V_n ($n = 3m$, $m = 1-7$), Nb_n ($n = 3m$, $m = 1-7$), and $Ti_nV_nNb_n$ ($n = 1-7$) systems is 1.24 0.86, 1.23, and 1.21 eV, respectively. The calculation results for VEA show that the titanium system has better electron trapping ability than other systems. Our calculation results can provide a theoretical reference for designing more efficient HEA catalysts.

CONCLUSIONS

We used both ESPR and BH-MRS methods to systematically explore the structure evolution process of Ti_n ($n = 3m$, $m = 1-7$), V_n ($n = 3m$, $m = 1-7$), Nb_n ($n = 3m$, $m = 1-7$), and $Ti_nV_nNb_n$ ($n = 1-7$) systems. We found that equiatomic $Ti_nV_nNb_n$ ($n = 1-7$) systems have similar lowest energy structures with the same size Ti_n ($n = 3m$, $m = 1-7$), V_n ($n = 3m$, $m = 1-7$), and Nb_n ($n = 3m$, $m = 1-7$) systems, and this indicates that the spatial position of different elements can be exchanged, which does not change their structure for the nanoparticles composed of titanium, vanadium, or niobium elements. This property is very important for us to design multicomponent nanoparticle structures, and it overcomes the

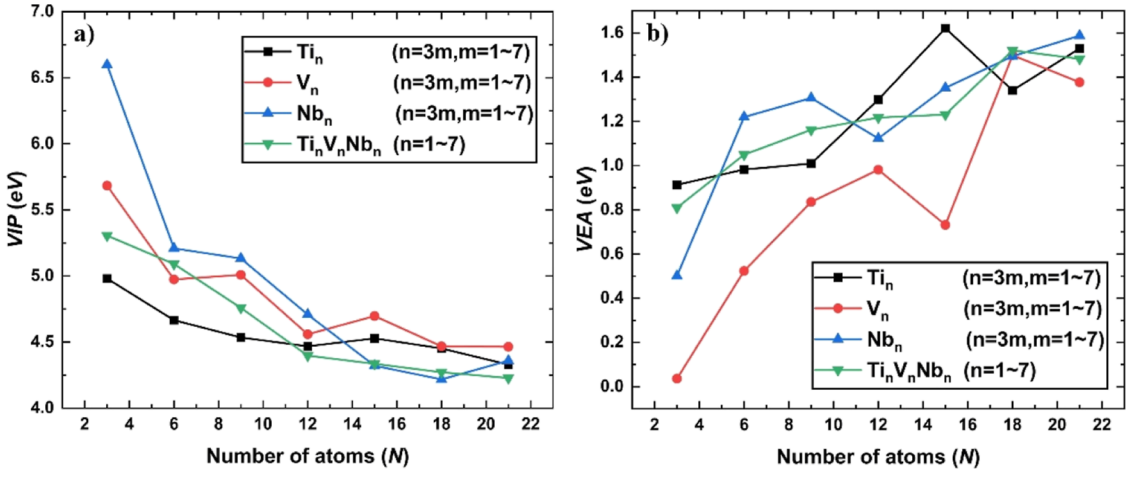

Figure 10. Electronic structural stability calculation for (a) VIP and (b) VEA. All of the calculations are based on GM structures of Ti_n ($n = 3m$, $m = 1-7$), V_n ($n = 3m$, $m = 1-7$), Nb_n ($n = 3m$, $m = 1-7$), and $Ti_nV_nNb_n$ ($n = 1-7$) systems.

https://doi.org/10.1021/acsomega.4c07777
ACS Omega 2024, 9, 45545−45553

shortcomings of traditional algorithms in searching the structure of multicomponent nanoparticles. By comparing the similarity of lowest energy structures of Ti_n ($n = 3m$, $m = 1-7$), V_n ($n = 3m$, $m = 1-7$), Nb_n ($n = 3m$, $m = 1-7$), and $Ti_nV_nNb_n$ ($n = 1-7$) systems, we found that more than 81% structure similarity values are greater than 0.9, and this further indicates that the multicomponent TiVNb system has the structure invariance for element exchange at the molecular level. For $Ti_7V_7Nb_7$ system searching, the average sampling step of the BH-MRS method is 1226 more than that of the ESPR method to find the six-ring layered structure. The electronic property calculation of Ti_n ($n = 3m$, $m = 1-7$), V_n ($n = 3m$, $m = 1-7$), Nb_n ($n = 3m$, $m = 1-7$), and $Ti_nV_nNb_n$ ($n = 1-7$) systems show that adding equiatomic vanadium and niobium elements to a pure titanium system may not change its stability, and the Ti_n ($n = 3m$, $m = 1-7$) system has better electron trapping ability than other systems. Finally, our study provides molecular level structural data for the design of HEAs with better mechanical and catalytic properties.

■ ASSOCIATED CONTENT

Supporting Information

The Supporting Information is available free of charge at https://pubs.acs.org/doi/10.1021/acsomega.4c07777.

All of the configuration information on lowest energy structures for Ti_n ($n = 3m$, $m = 1-7$), V_n ($n = 3m$, $m = 1-7$), Nb_n ($n = 3m$, $m = 1-7$), and $Ti_nV_nNb_n$ ($n = 1-7$) systems (PDF)

■ AUTHOR INFORMATION

Corresponding Author

Yi-Rong Liu − *Public Experimental Teaching Center, Panzhihua University, Panzhihua, Sichuan 61700, China;* orcid.org/0000-0002-2568-2728; Email: liuyirong@pzhu.edu.cn

Authors

Yan Jiang − *School of Vanadium and Titanium, Panzhihua University, Panzhihua, Sichuan 61700, China*

Lang Bai − *Public Experimental Teaching Center, Panzhihua University, Panzhihua, Sichuan 61700, China*

Complete contact information is available at: https://pubs.acs.org/10.1021/acsomega.4c07777

Author Contributions

Yi-Rong Liu constructed the method and analyzed the results. **Yan Jiang** prepared the manuscript. **Lang Bai** performed the part of the theoretical calculation.

Notes

The authors declare no competing financial interest.

■ ACKNOWLEDGMENTS

The study was supported by grants from the Sichuan Province Science and Technology Plan Project, Key Research and Development Project (No. 2023YFG0217), and National Natural Science Foundation of China (grant No. 41775112). Part of the computation was performed at the supercomputing Center of the Chinese Academy of Sciences and the Supercomputing Center of USTC.

■ REFERENCES

(1) Mirkin, C. A.; Letsinger, R. L.; Mucic, R. C.; Storhoff, J. J. A DNA-based method for rationally assembling nanoparticles into macroscopic materials. *Nature* **1996**, *382*, 607−609.

(2) Hong, B. H.; Bae, S. C.; Lee, C. W.; Jeong, S.; Kim, K. S. Ultrathin single-crystalline silver nanowire arrays formed in an ambient solution phase. *Science* **2001**, *294*, 348−351.

(3) Hakkinen, H.; Abbet, S.; Sanchez, A.; Heiz, U.; Landman, U. Structural, electronic, and impurity-doping effects in nanoscale chemistry: Supported gold nanoclusters. *Angew. Chem., Int. Ed.* **2003**, *42*, 1297−1300.

(4) Guvelioglu, G. H.; Ma, P. P.; He, X. Y.; Forrey, R. C.; Cheng, H. S. Evolution of small copper clusters and dissociative chemisorption of hydrogen. *Phys. Rev. Lett.* **2005**, *94*, 026103.

(5) Fernando, A.; Weerawardene, K. L. D. M.; Karimova, N. V.; Aikens, C. M.; Aikens, C. M. Quantum Mechanical Studies of Large Metal, Metal Oxide, and Metal Chalcogenide Nanoparticles and Clusters. *Chem. Rev.* **2015**, *115*, 6112−6216.

(6) Alonso, J. A. Electronic and atomic structure, and magnetism of transition-metal clusters. *Chem. Rev.* **2000**, *100*, 637−678.

(7) Yeh, J. W.; Chen, S. K.; Lin, S. J.; Gan, J. Y.; Chin, T. S.; Shun, T. T.; Tsau, C. H.; Chang, S. Y. Nanostructured high-entropy alloys with multiple principal elements: novel alloy design concepts and outcomes. *Adv. Eng. Mater.* **2004**, *6*, 299−303.

(8) Miracle, D. B.; Senkov, O. N. A critical review of high entropy alloys and related concepts. *Acta Mater.* **2017**, *122*, 448−511.

(9) George, E. P.; Raabe, D.; Ritchie, R. O. High-entropy alloys. *Nat. Rev. Mater.* **2019**, *4*, 515−534.

(10) Gludovatz, B.; Hohenwarter, A.; Catoor, D.; Chang, E. H.; George, E. P.; Ritchie, R. O. A fracture-resistant high-entropy alloy for cryogenic applications. *Science* **2014**, *345*, 1153−1158.

(11) Koželj, P.; Vrtnik, S.; Jelen, A.; Jazbec, S.; Jagličić, Z.; Maiti, S.; Feuerbacher, M.; Steurer, W.; Dolinšek, J. Discovery of a Superconducting High-Entropy Alloy. *Phys. Rev. Lett.* **2014**, *113*, 107001.

(12) Liu, S. R.; Zhai, H. J.; Castro, M.; Wang, L. S. Photoelectron spectroscopy of Ti_n^- clusters (n = 1−130). *J. Chem. Phys.* **2003**, *118*, 2108−2115.

(13) Sakurai, M.; Watanabe, K.; Sumiyama, K.; Suzuki, K. Magic numbers in transition metal (Fe, Ti, Zr, Nb, and Ta) clusters observed by time-of-flight mass spectrometry. *J. Chem. Phys.* **1999**, *111*, 235−238.

(14) Moskovits, M.; Srnova-Sloufova, I.; Vlckova, B. Bimetallic Ag-Au nanoparticles: Extracting meaningful optical constants from the surface-plasmon extinction spectrum. *J. Chem. Phys.* **2002**, *116*, 10435−10446.

(15) Jiang, Y.; Liu, Y. R. New Multicomponent Optimization Scheme for Equiatomic Vanadium-Titanium Nanoparticle Study. *J. Chem. Theory Comput.* **2023**, *19*, 8998−9007.

(16) King, D. J. M.; Middleburgh, S. C.; McGregor, A. G.; Cortie, M. B. Predicting the formation and stability of single phase high-entropy alloys. *Acta Mater.* **2016**, *104*, 172−179.

(17) Matusiak, K.; Berent, K.; Marciszko, M.; Cieslak, J. The experimental and theoretical study on influence of Al and Cu contents on phase abundance changes in Al Cu FeCrNiCo HEA system. *J. Alloys Compd.* **2019**, *790*, 837−846.

(18) Zhang, C.; Zhang, F.; Chen, S.; Cao, W. Computational Thermodynamics Aided High-Entropy Alloy Design. *JOM* **2012**, *64*, 839−845.

(19) Wu, C. T.; Chang, H. T.; Wu, C. Y.; Chen, S. W.; Huang, S. Y.; Huang, M. X.; Pan, Y. T.; Bradbury, P.; Chou, J.; Yen, H. W. Machine learning recommends affordable new Ti alloy with bone-like modulus. *Mater. Today* **2020**, *34*, 41−50.

(20) Li, R. X.; Xie, L.; Wang, W. Y.; Liaw, P. K.; Zhang, Y. High-Throughput Calculations for High-Entropy Alloys: A Brief Review. *Front. Mater.* **2020**, *7*, 290.

(21) Wales, D. J.; Doye, J. P. Global optimization by basin-hopping and the lowest energy structures of Lennard-Jones clusters containing up to 110 atoms. *J. Phys. Chem. A* **1997**, *101*, 5111−5116.

(22) Deaven, D. M.; Ho, K.-M. Molecular geometry optimization with a genetic algorithm. *Phys. Rev. Lett.* **1995**, *75*, 288−291.
(23) Kirkpatrick, S.; Gelatt, C. D., Jr; Vecchi, M. P. Optimization by simulated annealing. *Science* **1983**, *220*, 671−680.
(24) Lv, J.; Wang, Y.; Zhu, L.; Ma, Y. Particle-swarm structure prediction on clusters. *J. Chem. Phys.* **2012**, *137*, 084104.
(25) Liu, Y. R.; Jiang, Y.; Jiang, S.; Wang, C. Y.; Huang, T. Global minima optimization via mirror-rotation transformation. *Phys. Rev. Res.* **2022**, *4*, L042045.
(26) Senkov, O.; Scott, J.; Senkova, S.; Miracle, D.; Woodward, C. Microstructure and room temperature properties of a high-entropy TaNbHfZrTi alloy. *J. Alloys Compd.* **2011**, *509*, 6043−6048.
(27) Senkov, O.; Scott, J.; Senkova, S.; Meisenkothen, F.; Miracle, D.; Woodward, C. Microstructure and elevated temperature properties of a refractory TaNbHfZrTi alloy. *J. Mater. Sci.* **2012**, *47*, 4062−4074.
(28) Senkov, O.; Woodward, C. Microstructure and properties of a refractory NbCrMo0. 5Ta0. 5TiZr alloy. *Mater. Sci. Eng., A* **2011**, *529*, 311−320.
(29) Senkov, O. N.; Senkova, S. V.; Woodward, C.; Miracle, D. B. Low-density, refractory multi-principal element alloys of the Cr−Nb−Ti−V−Zr system: Microstructure and phase analysis. *Acta Mater.* **2013**, *61*, 1545−1557.
(30) Wu, Y.; Cai, Y.; Chen, X.; Wang, T.; Si, J.; Wang, L.; Wang, Y.; Hui, X. Phase composition and solid solution strengthening effect in TiZrNbMoV high-entropy alloys. *Mater. Des.* **2015**, *83*, 651−660.
(31) Guo, N.; Wang, L.; Luo, L.; Li, X.; Su, Y.; Guo, J.; Fu, H. Microstructure and mechanical properties of refractory MoNbHfZrTi high-entropy alloy. *Mater. Des.* **2015**, *81*, 87−94.
(32) Schebarchov, D.; Wales, D. J. Structure Prediction for Multicomponent Materials Using Biminima. *Phys. Rev. Lett.* **2014**, *113*, 156102.
(33) Perdew, J. P.; Burke, K.; Ernzerhof, M. Generalized gradient approximation made simple. *Phys. Rev. Lett.* **1996**, *77*, 3865−3868.
(34) Delley, B. An All-Electron Numerical-Method for Solving the Local Density Functional for Polyatomic-Molecules. *J. Chem. Phys.* **1990**, *92*, 508−517.
(35) Neese, F. The ORCA program system. *Wiley Interdiscip. Rev.: Comput. Mol. Sci.* **2012**, *2*, 73−78.
(36) Zhao, Y. F.; Chen, X.; Li, J. TGMin: A global-minimum structure search program based on a constrained basin-hopping algorithm. *Nano Res.* **2017**, *10*, 3407−3420.
(37) Ballester, P. J.; Richards, W. G. Ultrafast shape recognition to search compound databases for similar molecular shapes. *J. Comput. Chem.* **2007**, *28*, 1711−1723.
(38) Ballester, P. J.; Richards, W. G. Ultrafast shape recognition for similarity search in molecular databases. *Proc. R. Soc. A* **2007**, *463*, 1307−1321.
(39) Ballester, P. J.; Finn, P. W.; Richards, W. G. Ultrafast shape recognition: evaluating a new ligand-based virtual screening technology. *J. Mol. Graph. Model.* **2009**, *27*, 836−845.
(40) Liu, Y. R.; Wen, H.; Huang, T.; Lin, X. X.; Gai, Y. B.; Hu, C. J.; Zhang, W. J.; Huang, W. Structural Exploration of Water, Nitrate/Water, and Oxalate/Water Clusters with Basin-Hopping Method Using a Compressed Sampling Technique. *J. Phys. Chem. A* **2014**, *118*, 508−516.
(41) Liu, Y.-R.; Jiang, Y. Growth mechanism prediction for nanoparticles via structure matching polymerization. *Phys. Chem. Chem. Phys.* **2024**, *26*, 1267−1273.
(42) Yao, Y.; Dong, Q.; Brozena, A.; Luo, J.; Miao, J.; Chi, M.; Wang, C.; Kevrekidis, I. G.; Ren, Z. J.; Greeley, J.; et al. High-entropy nanoparticles: Synthesis-structure-property relationships and data-driven discovery. *Science* **2022**, *376*, No. eabn3103.
(43) Li, H.; Lai, J.; Li, Z.; Wang, L. Multi-sites electrocatalysis in high-entropy alloys. *Adv. Funct. Mater.* **2021**, *31*, 2106715.
(44) Chen, Z. W.; Li, J.; Ou, P.; Huang, J. E.; Wen, Z.; Chen, L.; Yao, X.; Cai, G.; Yang, C. C.; Singh, C. V.; et al. Unusual Sabatier principle on high entropy alloy catalysts for hydrogen evolution reactions. *Nat. Commun.* **2024**, *15*, 359.
(45) Subhash, B.; Unocic, R. R.; Lie, W. H.; Gallington, L. C.; Wright, J.; Cheong, S.; Tilley, R. D.; Bedford, N. M. Resolving Atomic-Scale Structure and Chemical Coordination in High-Entropy Alloy Electrocatalysts for Structure−Function Relationship Elucidation. *ACS Nano* **2023**, *17*, 22299−22312.

https://doi.org/10.1021/acsomega.4c07777
ACS Omega 2024, 9, 45545−45553